ELSEVIER

Journal of Environmental Management 85 (2007) 574–584

Journal of Environmental Management

www.elsevier.com/locate/jenvman

Observation and simulation of net primary productivity in Qilian Mountain, western China

Y. Zhou[a,b,*], Q. Zhu[a], J.M. Chen[c], Y.Q. Wang[b], J. Liu[d], R. Sun[a], S. Tang[a]

[a]*College of Geography and Remote Sensing, Beijing Normal University, China*
[b]*Department of Natural Resources Science, University of Rhode Island, Kingston, RI 02881, USA*
[c]*Department of Geography and Program in Planning, University of Toronto, 100 St. George Street, Room 5047, Toronto, Ont., Canada M5S 3G3*
[d]*Department of Physics, University of Toronto, Canada*

Received 4 April 2005; received in revised form 12 December 2005; accepted 3 April 2006
Available online 28 November 2006

Abstract

We modeled net primary productivity (NPP) at high spatial resolution using an advanced spaceborne thermal emission and reflection radiometer (ASTER) image of a Qilian Mountain study area using the boreal ecosystem productivity simulator (BEPS). Two key driving variables of the model, leaf area index (LAI) and land cover type, were derived from ASTER and moderate resolution imaging spectroradiometer (MODIS) data. Other spatially explicit inputs included daily meteorological data (radiation, precipitation, temperature, humidity), available soil water holding capacity (AWC), and forest biomass. NPP was estimated for coniferous forests and other land cover types in the study area. The result showed that NPP of coniferous forests in the study area was about 4.4 $tC\,ha^{-1}\,y^{-1}$. The correlation coefficient between the modeled NPP and ground measurements was 0.84, with a mean relative error of about 13.9%.

Keywords: BEPS; Biomass; Leaf area index; Net primary productivity; Western China

1. Introduction

The terrestrial carbon cycle is an important issue in global change research in the International Geosphere–Biosphere Programme (IGBP) (Geng et al., 2000). In recent years, modeling the net primary productivity (NPP) of terrestrial ecosystems has been a subject of increasing interest because of the importance of the terrestrial carbon cycle in the global carbon budget and climate change (Chen et al., 1999a). NPP is defined as the net amount of new carbon absorbed by plants per unit of space and time (Liu et al., 1999). NPP indicates the growth status of vegetation, and provides the information for the management of renewable biological resources.

Measurement and simulation of global and regional NPP are among important research subjects in carbon cycle studies. In order to carry out NPP measurement and simulation over large areas, different NPP models have been developed over the last two decades. Those include statistical models, climate-based models, process models, and energy use efficiency models (Zheng and Zhou, 2000; Luo et al., 1998; Chen et al., 1999; Piao et al., 2001). Remote sensing data have been frequently used in global change studies. The NPP models, augmented by remote sensing data and Geographic Information Systems (GIS), help to acquire representative NPP information at regional and global scales.

Statistical NPP models are mainly based on remote sensing data and in situ observations. Remote-sensing-based models quantify the relationship between vegetation indices and NPP (Xiao et al., 1996; Zheng and Zhou, 2000). In situ-based models use field measurements to scale NPP from sites to regions (Luo et al., 1998; Zhou et al., 2002; Ni, 2003). These models, although easy to operate, lack broad applicability and need measured NPP to establish the relationship.

Several climate-based models have been reported, e.g., Miami model, Montreal model, Beijing model, and others

*Corresponding author. Department of Natural Resources Science, University of Rhode Island, Kingston, RI 02881, USA. Tel.: +1 401 874 9035; fax: +1 401 874 4561.
E-mail address: ilikespoon@mail.uri.edu (Y. Zhou).

0301-4797/$ - see front matter © 2006 Elsevier Ltd. All rights reserved.
doi:10.1016/j.jenvman.2006.04.024

(Li et al., 1998; Zhou and Zhang, 1995; Zhu, 1993; Ni, 1996). These models quantify the relationships between NPP and meteorological data or other derivative variables in the study areas. NPP derived by these models is considered potential NPP because these models assume dense vegetation canopies and consider climatic parameters only. In addition, the above models cannot produce the variation in NPP within a year because they use only annual-average data.

The Carnegie-Ames-Stanford Approach (CASA) model has been often used as the energy use efficiency model in global and regional NPP estimations (Piao et al., 2001; Ke et al., 2003; Piao and Fang, 2002; Chen et al., 2001, 2002a, b; Field et al., 1995). Other energy use efficiency models have also been used to obtain the spatial distribution of NPP (Ahl et al., 2004; Choudhury, 2002; Furumi et al., 2002; Sun and Zhu, 2000, 2001; Goetz and Prince, 1996; Gower et al., 1999). Similar to energy use efficiency models, global NPP was obtained using carbon use-efficiency and model-obtained GPP (Choudhury, 2000). These models employ the fraction of photosynthetically active radiation (FPAR) absorbed by vegetation (that could be estimated from vegetation indices) and light use efficiencies to obtain the increments of dry matter. Compared with process models, the energy use efficiency models are relatively simple and can incorporate remote sensing data easily. However, the light use efficiency, an important parameter in these models, changes with vegetation type as well as with time for the same vegetation type.

Process models, for example FOREST_BGC, DEMETER, TEM, CENTURY, FBM, BEPS, describe the key ecosystem processes and simulate the dependency of NPP on one of the main interacting processes according to physiological and ecological principles (Zhang et al., 2003a, b; Reich et al., 1999; Coops et al., 2001; Jiang et al., 1999; Chen et al., 2003). Because the time interval of process models is generally short, these models can estimate NPP over longer periods through the integration of gross photosynthesis within short time periods. Most process models have several parameters, some of which can only be obtained by ground measurements, and others are empirical or semi-empirical. However, although process models are somewhat complex and need more input parameters, they have many advantages such as the ability to handle interactions and feedbacks among different processes.

As a process model, the BEPS is unique in the integration of instantaneous gross photosynthesis by considering the general diurnal patterns of meteorological variables as well as in separating the canopy leaves into sunlit and shaded groups. Remote sensing data are used in the BEPS to acquire the spatial distribution of LAI, land cover type, and biomass. The difference between BEPS and some other NPP models, such as climate-based models, is that BEPS model can be used to obtain an accurate spatial distribution of NPP. It has been used widely in many geographical locations and at different scales (Liu et al., 1997, 1999, 2002; Bunkei and Masayuki, 2002). Since most of the reported research in NPP simulations has employed coarse spatial resolution remote sensing data, the results are difficult to validate. However, it is now feasible to obtain high spatial resolution NPP to check the model and to validate the coarse resolution NPP estimates. With improved sensor systems, higher spatial resolution and frequent remote sensing observations have become available. However, the extension of site level NPP estimations using fine spatial resolution data is still a challenging research subject. In this study, we tested the possibility of using high spatial resolution ASTER data incorporated with high temporal resolution MODIS data in the BEPS model to simulate NPP in a coniferous forest-dominated area in Western China.

2. Methods

2.1. Study site

The study site is situated in the Qilian Mountain area centered at 38.7°N and 99.55°E within Gansu province, western China (Fig. 1). The elevation varies from 2200 to 4800 m above the sea level. The area has a temperate continental mountainous climate. In winter the atmospheric circulation is controlled by the Mongolia anticyclone; the conditions are cold and dry, with little precipitation. When the atmospheric circulation is controlled by the continental cyclone in the summer, the diurnal difference of temperature is dramatic. The difference of precipitation between summer and winter is large, and annual precipitation takes place mainly in the summer. Influenced by the climate and the terrain, the prevalent vegetation types in the study area are mountainous pastures and forests. The dominant vegetation includes *Picea crassifolia*, *Sabina przewalski*, and grassland. Vegetation density varies with terrain, soil, water, and climate factors. This site is ideal for the development of remote sensing biophysical parameters models because of the varieties of environmental factors. To validate the modeled NPP result, ground measurements of NPP were made in the study area in 2003.

2.2. Data source and data preparation

2.2.1. Leaf area index and vegetation index

After consideration of vegetation types, sample distributions and accessibility, 16 sites, mainly distributed in forested areas (Fig. 1), were selected for ground LAI measurements. The vegetation types in the selected sites represent the dynamic range of LAI so that the relationship between LAI and a vegetation index can be established. LAI was measured by the Tracing Radiation and Architecture of Canopies (TRAC) instrument. TRAC can be used to acquire the clumping index, which is an important factor for the LAI calculation of coniferous forests. The LAI measurements focused on *P. crassifolia*.

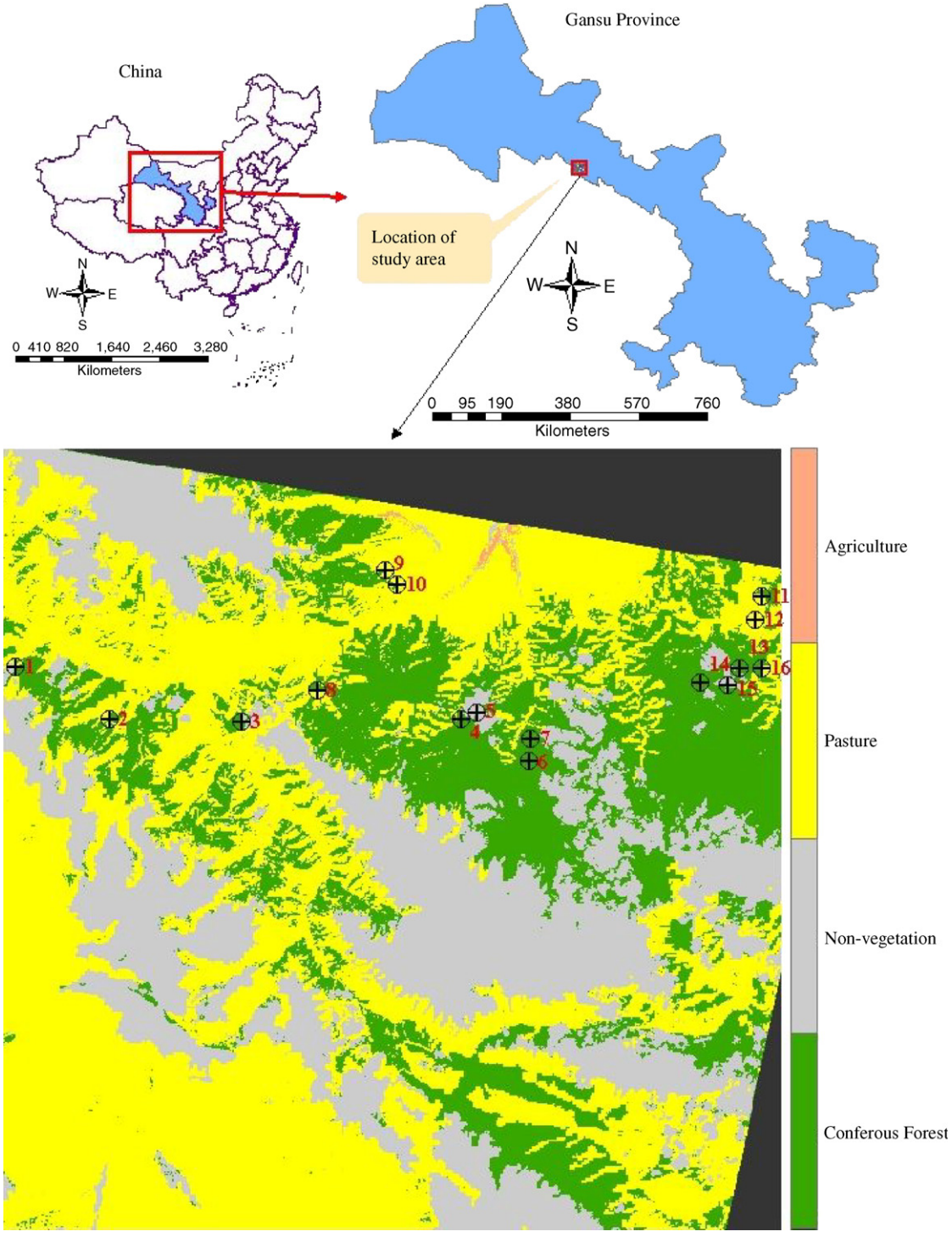

Fig. 1. Land cover map of the study area and locations of sampling sites.

The measured LAI ranged between 2.5 and 6 (Fig. 2, Table 1). The results reflect the vegetation conditions at the sites, and they provide the necessary information to establish a relationship with a vegetation index.

To decide which vegetation index should be used in this study, the simple ratio (SR), which is the ratio between near infrared and visible red spectral bands (R_{Nir}/R_{Red}), and the Normalized Difference Vegetation Index (NDVI) were compared and evaluated based on the established relationships with measured LAI. Based on this comparison, SR was selected as the vegetation index to be obtained from the satellite data.

2.2.2. *Ground measurements of biomass*

The relative growth method (Feng et al., 1998) was used to measure the biomass of coniferous forests. The biomass

of a tree includes components of the stem, branches, leaves, and roots. The biomass of each individual tree was estimated from tree height and diameter at breast height (DBH) using the species-specific relative growth formula by Feng et al. (1998). Recorded structural parameters included the number of trees in each sampling area and the DBH and height of each tree measured, and the tree biomass was calculated accordingly. The biomass at each site was calculated with the help of the number of trees. Only 15 sites were selected to make the biomass measurements because the last site (site 16) did not have all the data for biomass calculations. The measured biomass ranged between 60 and 200 tDW ha^{-1} (Fig. 3, Table 1). The sites with better soil, climate and terrain conditions have a higher accumulation of biomass, thus the field measurements reflect the ground and vegetation conditions well.

Eq. (1) was built and used to evaluate the errors contributed from different components of the biomass calculation:

$$\Delta W = \sum_{i=1}^{4}\left(\frac{\partial W_i}{\partial N_i}\Delta N + \frac{\partial W_i}{\partial D_i}\Delta D + \frac{\partial W_i}{\partial H_i}\Delta H\right),$$
$$\frac{\partial W_i}{\partial N_i} = a_i(D^2H)b_i/90,$$
$$\frac{\partial W_i}{\partial D_i} = 2Na_ib_iH^{b_i}D^{2b_i-1}/90,$$
$$\frac{\partial W_i}{\partial H_i} = Na_ib_iH^{b_i-1}(D)^{2b_i}/90, \quad (1)$$

where i represents different components of biomass (branch, stem, leaf, root); D is the DBH; H the tree height; N the number of trees in the sample area; a_i and b_i are the parameters in the relative growth equation. The sampling area is assumed 30 m × 30 m and all biomass components are in tDW ha^{-1}.

Fig. 4 illustrates the estimated errors of measured biomass for the sampled sites. DBH and height of trees contributed similar errors, and the number of trees in a

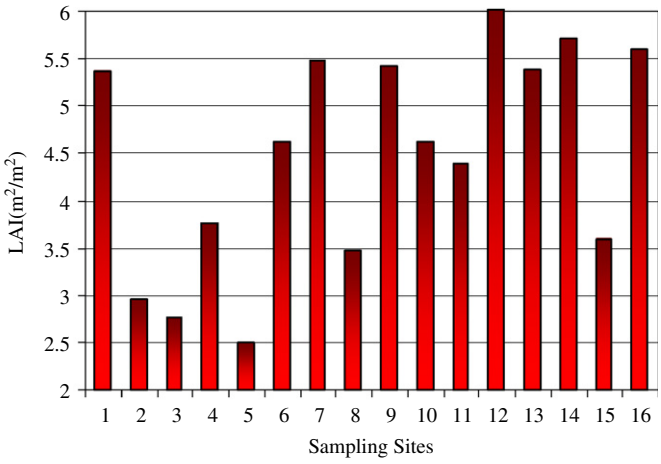

Fig. 2. Ground measurement of LAI in the sampling sites.

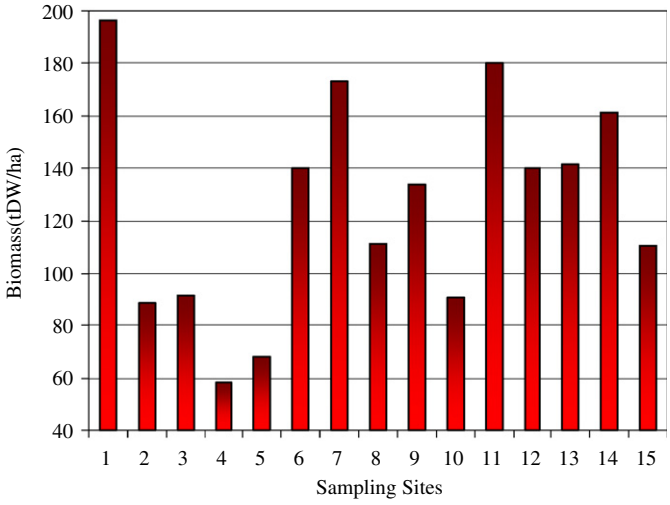

Fig. 3. Ground measurement of Biomass in the sampling sites.

Table 1
Site features and ground measurements of LAI, biomass and NPP of coniferous forests in the sampling sites

Site	Dem (m)	Size (m)	LAI	Biomass (tDW ha^{-1})	NPP (tC ha^{-1} a^{-1})
1	3034.0	30 × 30	5.36	196.67	5.50
2	2822.6	30 × 30	2.95	88.52	3.06
3	2859.3	15 × 15	2.76	91.70	3.73
4	2682.4	20 × 20	3.76	58.27	4.17
5	2737.2	20 × 20	2.49	68.22	2.62
6	2663.8	20 × 20	4.62	140.00	4.15
7	2643.6	20 × 20	5.49	173.32	5.23
8	2620.4	20 × 20	3.48	111.07	3.83
9	2748.8	30 × 30	5.42	133.61	4.86
10	2744.6	20 × 20	4.62	90.44	3.37
11	2839.2	20 × 20	4.39	180.05	5.36
12	2885.4	20 × 20	6.02	140.30	4.70
13	2966.0	30 × 30	5.39	141.74	3.98
14	2932.8	20 × 20	5.72	161.28	4.73
15	2890.2	30 × 30	3.58	110.61	3.07

sampling area contributed relatively small errors. The total errors of measured biomass ranged between 14 and 45 tDW ha^{-1}.

2.2.3. Ground measurements of NPP

NPP includes three components: change in live biomass, mortality, and the biomass consumed by animals (Feng et al., 1998). Since the last component accounts for a negligible amount of the total NPP, it is not considered in this study. Tree mortality is affected by stand age and other factors, and it can account for a significant fraction of the annual biomass increment. However, since remote-sensing-based estimation does not include the reduction of NPP due to mortality, this component is not considered either. The exclusion of this component enabled us to use ground measurement data to validate modeled results from remote sensing observations.

Our NPP measurements were conducted for coniferous forests only. The biomass increment data derived from the increment of DBH were used to calculate NPP. The DBH increment data were obtained from tree ring samples. Structural parameters of the sampled sites were recorded as described above. For each sampled site, 15 tree cores were obtained. The DBH increment data were then used to estimate the increment of the biomass component of each tree from 2000 to 2001 by the relative growth formula (Feng et al., 1998). The NPP of a site, or the change of biomass, was then estimated with the help of the number of trees in the sampling area. The results of ground NPP measurements are shown in Fig. 5 and Table 1. The measured NPP ranges between 3 and 7 tC ha^{-1} a^{-1}.

Eq. (2) was built and used to evaluate the errors contributed from different components of the NPP calculation:

$$\Delta \mathrm{NPP} = \sum_{i=1}^{4}\left(\frac{\partial \mathrm{NPP}_i}{\partial N_i}\Delta N + \frac{\partial \mathrm{NPP}_i}{\partial D_i}\Delta D + \frac{\partial \mathrm{NPP}_i}{\partial H_i}\Delta H + \frac{\partial \mathrm{NPP}_i}{\partial R_i}\Delta R\right),$$

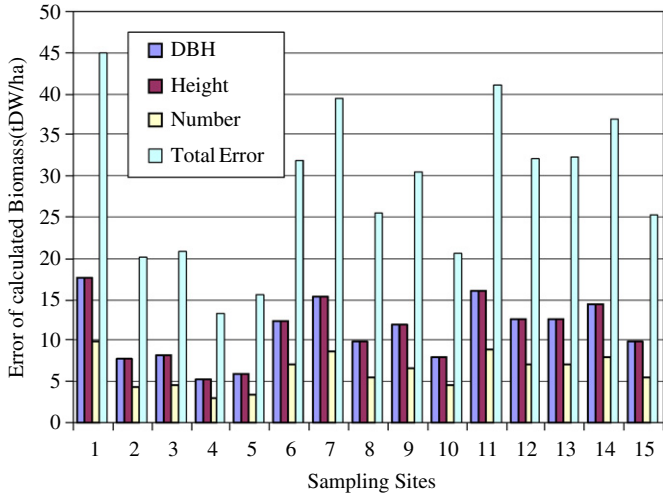

Fig. 4. Ground measurement errors of Biomass from each component in the sampling sites.

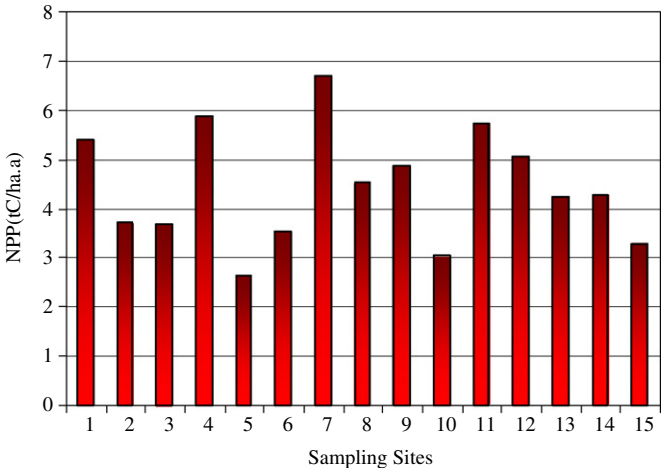

Fig. 5. Ground measurement result of NPP in the sampling sites.

$$\frac{\partial \mathrm{NPP}_i}{\partial N_i} = (a_i[D^2H]^{b_i} - a_i[(D-2R)^2H]^{b_i})/90,$$
$$\frac{\partial \mathrm{NPP}_i}{\partial D_i} = Na_iH^{b_i}(2b_i(D)^{2b_i-1} - 2b_i(D-2R)^{2b_i-1})/90,$$
$$\frac{\partial \mathrm{NPP}_i}{\partial H_i} = Na_ib_iH^{b_i-1}((D)^{2b_i} - (D-2R)^{2b_i})/90,$$
$$\frac{\partial \mathrm{NPP}_i}{\partial R_i} = 4Na_ib_iH^{b_i}(D-2R)^{2b_i-1}/90, \quad (2)$$

where i represents contribution to NPP from different components (branch, stem, leaf, root); D the DBH; H the tree height; N the number of trees in the sample area; R the width of a tree ring; a_i and b_i are the parameters in the relative growth equation. The sampling area is assumed 30 m × 30 m and the measurement unit is tC ha^{-1} a^{-1}.

Fig. 6 illustrates the estimated errors of measured NPP for the sites. It indicates that height of trees and width of tree rings contributed more errors than DBH and the number of trees in a sampled area. The total error of measured NPP ranged between 0.7 and 1.5 tC ha^{-1} a^{-1}.

2.2.4. Remote sensing data

Remote sensing images used in this study include ASTER and MODIS products of LAI. The ASTER data, acquired on 12 July 2001, have a 15 m spatial resolution and 14 spectral bands from the visible to the infrared portions of the electromagnetic spectrum. Two of the spectral bands in red and near-infrared were used to establish the relationship between LAI and a vegetation index SR. This high-resolution image was essential for directly validating modeled NPP against ground data. Atmospheric corrections were performed using the 6S software (http://www.ltid.inpe.br/dsr/mauro/6s/), using near real-time inputs of the precipitable water content and aerosol optical thickness from MODIS data products. After the atmospheric correction the ASTER image was georeferenced to Universal Transverse Mercator (UTM) map projection.

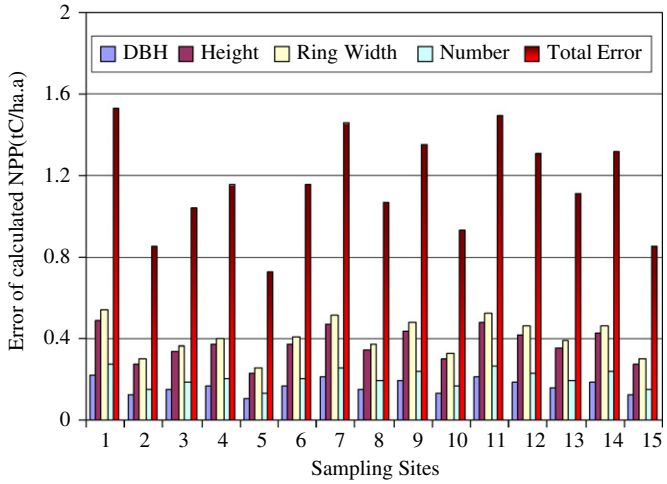

Fig. 6. Ground measurement errors of NPP from each component in the sampling sites.

A supervised classification was employed to classify the ASTER image. The final classification product had four categories: coniferous forests, pasture, agriculture, and non-vegetation (Fig. 1). The non-vegetation class included water and urban areas. With this land cover map, a relationship between LAI and SR for each vegetation type could be established.

In order to estimate NPP in 2001 using the BEPS model, the vegetation and environmental conditions of the study area for 2001 and 2003 were compared according to the local data. It was found that the vegetation types and LAI of the sample sites did not change substantially between 2001 and 2003. Therefore, the ground-measured coniferous forest LAI in 2003 was used to establish the relationship between LAI and SR in 2001.

For pasture and agriculture the LAI was not measured. A relationship between LAI and SR for these vegetation types was found from an existing work (Chen, 2002b):

$$\mathrm{LAI} = -1.6 \times \mathrm{LN}[(14.5 - \mathrm{SR})/13.5]. \quad (3)$$

The relationship in Eq. (3) was established using TM images. Since there was little spectral difference between selected ASTER and TM bands for SR, Eq. (3) was adopted for this study without modification.

It should be pointed out that the annual NPP cannot be modeled using a single LAI image. However, it is practically impossible to acquire high spatial resolution remote sensing data to derive LAI with the required temporal resolution. To solve this problem, MODIS LAI products for 2001 at 1 km resolution were used to provide the temporal information. MODIS LAI in a 10-day interval from Day 111 (April 21, 2001) to Day 294 (October 21, 2001) was obtained. It was assumed that LAI before Day 111 and after Day 294 had little variation, and therefore 20 MODIS LAI images between these two dates were used for the full annual cycle.

Matching LAI from MODIS to that at a finer spatial resolution is a challenging research subject (Chen, 1999; Tian et al., 2002a, b), involving complex scaling issues that are beyond the scope of this paper. Therefore, this study assumed that the temporal trend of LAI from MODIS is the same as that at a finer resolution. It was recognized that there was much uncertainty in MODIS LAI temporal trend for each 1 km pixel. Therefore, MODIS temporal trends were averaged for each vegetation type according to the land cover map derived from the ASTER image. The seasonal variation pattern derived from the MODIS LAI series for each vegetation type was then superimposed on the ASTER LAI image by preserving both LAI values in the ASTER image and the MODIS seasonal pattern. In this way, high spatial resolution LAI images corresponding to the days between April 21 and October 31, 2001 in ten-day intervals were derived (Fig. 7).

2.3. Model description

The NPP simulated by BEPS using the ASTER data is useful in three ways. Firstly, it can test the application of BEPS at a high spatial resolution. Secondly, the result of NPP can be used to validate the spatial distribution of NPP in products with a coarser spatial resolution. Thirdly, the modeled NPP using ASTER image can be directly validated through ground measurements.

In BEPS, NPP is estimated from gross primary productivity (GPP) and autotrophic respiration (R_a) as follows (Eq. (4)–(6), Liu et al., 2002):

$$\mathrm{NPP} = \mathrm{GPP} - R_a, \quad (4)$$

$$\mathrm{GPP} = (A_{\mathrm{sun}}\,\mathrm{LAI}_{\mathrm{sun}} + A_{\mathrm{shade}}\,\mathrm{LAI}_{\mathrm{shade}})\mathrm{Day\_Length\ Factor}, \quad (5)$$

$$R_a = R_m + R_g, \quad (6)$$

where the subscripts 'sun' and 'shade' denote the sunlit and shaded components of daily mean photosynthesis rate (A) and LAI. Factor converts GPP unit into $\mathrm{g\,C\,m^{-2}\,day^{-1}}$. Daily R_a is autotrophic respiration, R_m is maintenance respiration, and R_g is growth respiration.

Since the original BEPS model was designed for the analysis of boreal ecosystems, we modified it in this study to test its application using high spatial resolution remote sensing images in coniferous forests. The clumping index was taken into account for the sample sites due to its importance in the calculation of sunlit NPP and shaded NPP.

2.4. Input parameters for BEPS

The main inputs to BEPS include land cover type, available soil water capacity (AWC), biomass, LAI, and meteorological data. Meteorological data, including daily maximum and minimum air temperature, vapor pressure deficit, and precipitation for 2001, were obtained from 22 meteorological stations adjacent to the study site. Because of the rough terrain in the study area, the impact of

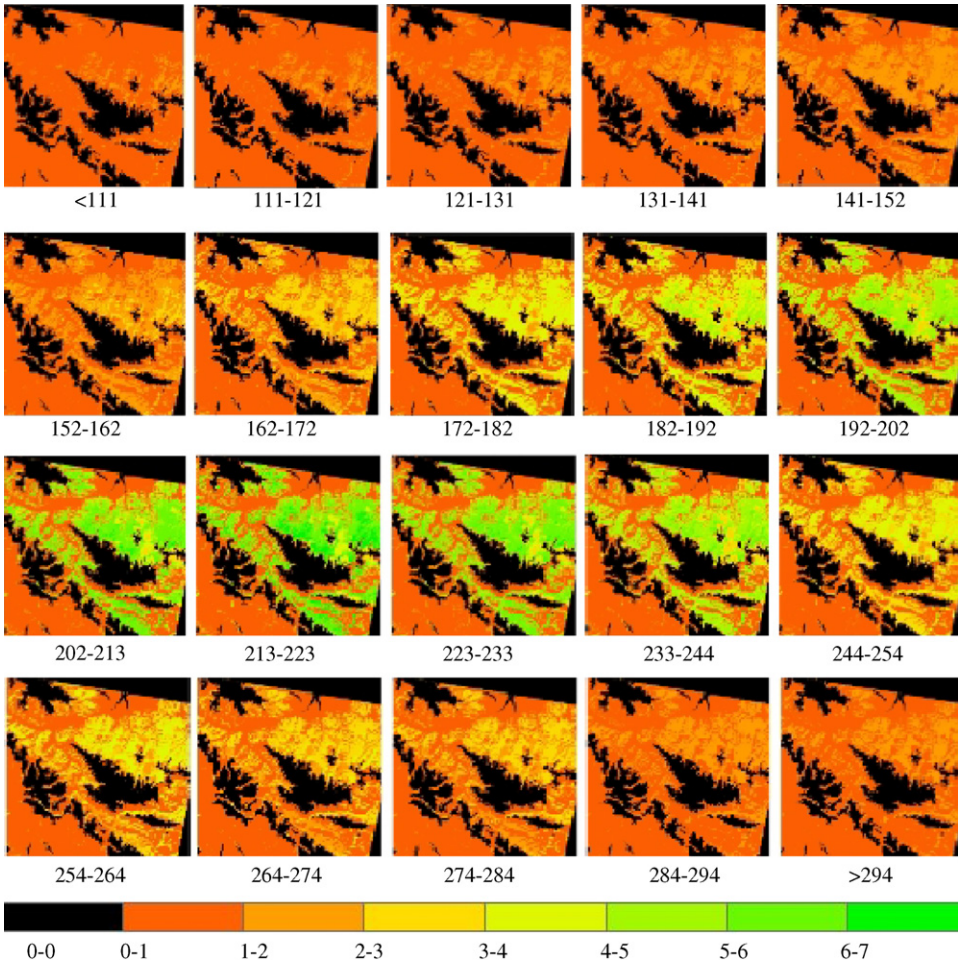

Fig. 7. Temporal change LAI with 15 m spatial resolution in 2001 (the number below the picture is the Julian day).

topographic conditions in the interpolation of the meteorological data had to be considered. The ANUSPLIN software (http://cres.anu.edu.au), proven to be appropriate for spatial interpolation of climate, was used to interpolate the meteorological data with terrain information. Data from the 22 stations were therefore interpolated by ANUSPLIN to 1 km resolution based on a digital terrain model, and further interpolated to 15 m resolution using a bilinear interpolation function within BEPS.

Global radiation is an important parameter required in the BEPS model. Since radiation data from meteorological stations are limited, data from the National Center for Atmospheric Research (NCAR) (http://www.ncar.ucar.edu/) was adopted for data enhancement. The relationship between NCAR global radiation ($S_{g,\ NCAR}$) data and the meteorological station ($S_{g,\ meteorological\ stations}$) data was established (Eq. (7), Fig. 8), and NCAR radiation fields were corrected before use in the BEPS model:

$$S_{g,meteorological\text{-}stations} = 0.6407 * S_{g,}\ NCAR. \quad (7)$$

Soil AWC was estimated according to the information provided in a 1:250,000 soil texture map. Above-ground forest biomass is important in BEPS for estimating maintenance respiration of vegetation. To acquire the

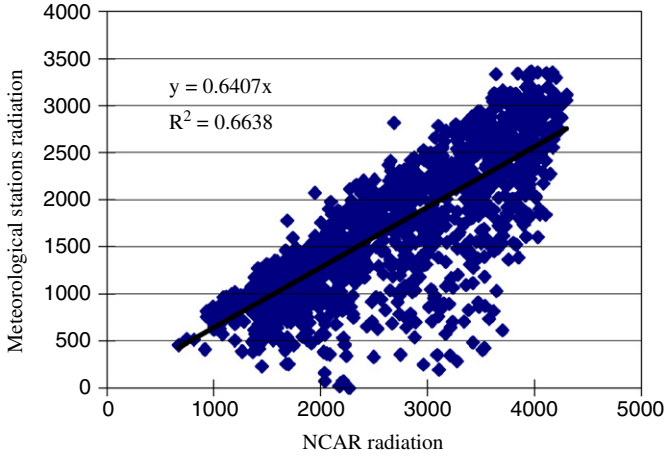

Fig. 8. Relationship between radiation from NCAR and meteorological stations.

spatial distribution of biomass in the study area, the observed biomass and measured LAI data for coniferous forests were used to establish their relationship (Eq. (8), Fig. 9):

$$W = 31.059 * LAI^{0.9275}, \quad (8)$$

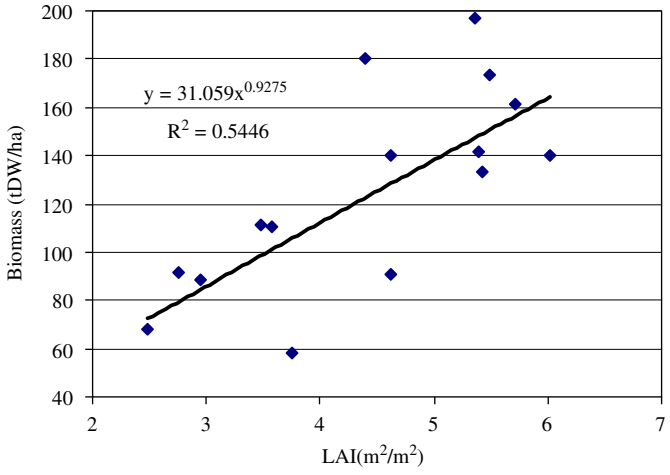

Fig. 9. Relationship between measured biomass and LAI.

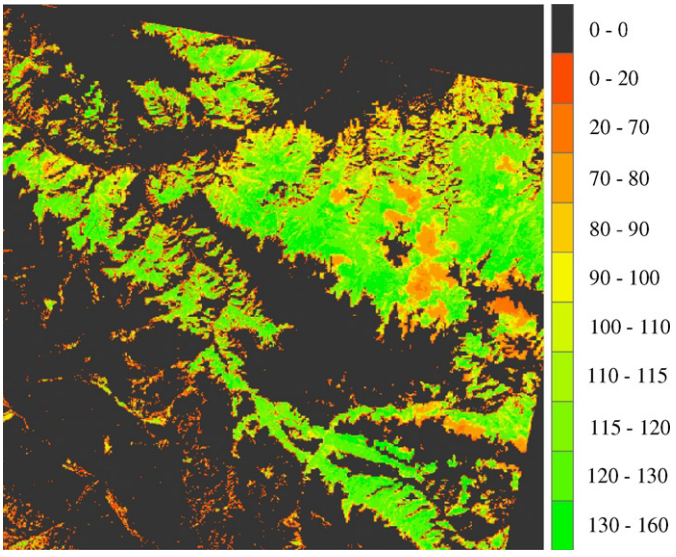

Fig. 10. Biomass (tDW ha^{-1}) distribution from LAI.

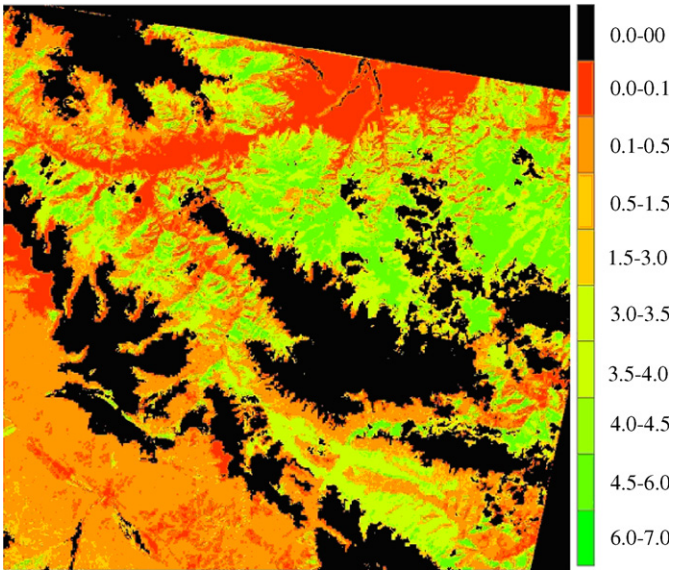

Fig. 11. Modeled NPP (tC ha^{-1} a^{-1}) in 2001 in the study area.

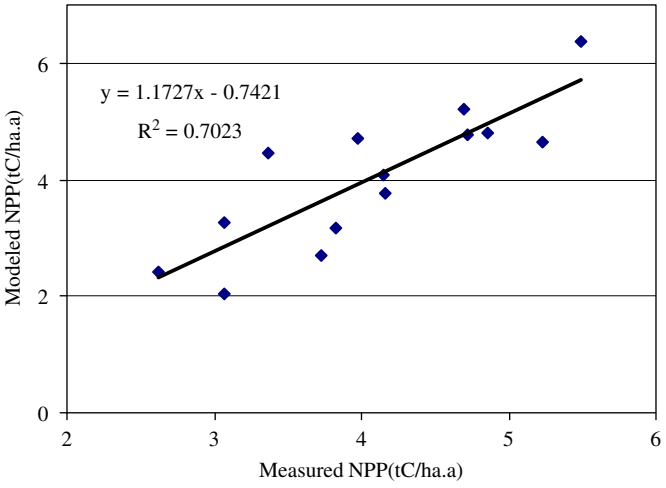

Fig. 12. Comparison of ground measured NPP and BEPS-modeled NPP.

where W is above-ground forest biomass (tDW ha^{-1}). The unit of W is further converted into tC ha^{-1} by multiplying the factor 0.5. This relationship was applied to the LAI image, thus obtaining the distribution of coniferous forest biomass (Fig. 10).

3. Results

Using the BEPS model and the input data, the NPP for 2001 was estimated in the study area. Its spatial pattern is illustrated in Fig. 11. The annual NPP of the coniferous forests mainly ranges between 2 and 7 tC ha^{-1} a^{-1}, and the mean annual NPP is about 4.4 tC ha^{-1} a^{-1}. The modeled result in Fig. 11 indicates that the coniferous forest yields greater NPP than the pasture. The variance of NPP reflects the differences in ground conditions such as terrain and climate.

Fourteen out of the 15 sampled sites were used to carry out the analysis of correlation and relative errors; site 11 was excluded due to cloud cover in the ASTER image. The comparison between modeled NPP and ground measurements indicates that the modeled NPP was consistent and comparable with the ground measured NPP. The correlation coefficient between these two sets of NPP results was 0.84 (Fig. 12). The modeled and measured NPP have a similar range of between 2 and 7 tC ha^{-1} a^{-1} for the study area. The mean relative error (MRE) was 13.9%, calculated using Eq. (9):

$$\mathrm{MRE} = \frac{1}{n}\sum_{i=1}^{n}\frac{\left|\mathrm{NPP}_{(\mathrm{measured},\,i)} - \mathrm{NPP}_{(\mathrm{modeled},\,i)}\right|}{\mathrm{NPP}_{(\mathrm{measured},\,i)}} \times 100\%, \tag{9}$$

where n is the number of sample sites; $\mathrm{NPP}_{(\mathrm{measured},\,i)}$ is the measured NPP of the ith site; $\mathrm{NPP}_{(\mathrm{modeled},\,i)}$ is the modeled NPP of the ith site.

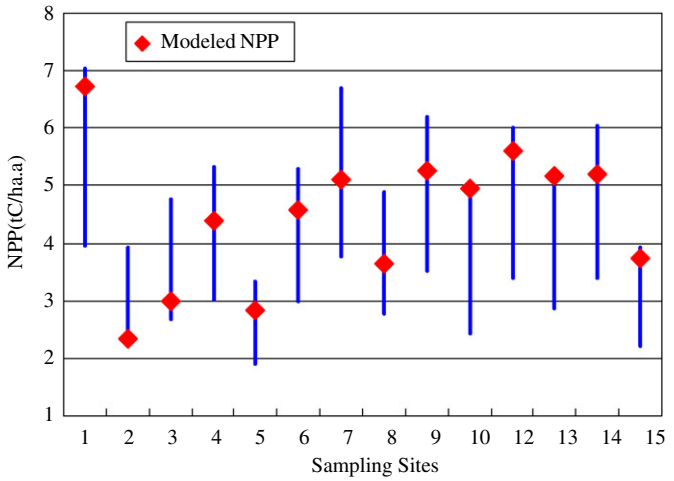

Fig. 13. Comparison of ground measured NPP range and BEPS-modeled NPP.

The comparison between modeled NPP and the range of measured NPP are illustrated in Fig. 13. It shows that the modeled NPP in all the 14 sites was within the range of measured NPP. The modeled NPP tends to occur near the upper limit of the measured range at sites 1, 10, 12, 13, and 15, while at sites 2 and 3 it is shifted in the opposite direction (Fig. 13). These differences may have resulted from errors in input data to the model and in ground NPP measurements.

Because LAI and above ground biomass of coniferous forests are not well correlated, the difference between the predicted biomass via LAI and measured biomass was compared with the difference between the modeled and measured NPP. The result indicated that there was no significant relationship between these two differences. Therefore, the error between modeled and measured NPP did not have much relationship with spatial variation of biomass independent of LAI variation.

4. Discussion and conclusions

LAI of the coniferous forests in this area ranges between 2.5 and 6. Since these forests were purely coniferous, the measurement error was smaller compared with that of mixed forests. This is advantageous for obtaining LAI images for NPP simulation. The measured biomass ranged between 60 and 200 $tDW\,ha^{-1}$, which has a similar distribution among the sampled sites as the ground measured LAI. The measured NPP ranged between 3 and 7 $tC\,ha^{-1}\,a^{-1}$. The ground measurements of NPP in the sampling sites possess a similar pattern as the measured LAI and biomass (Figs. 2 and 3). However, the differences of measured NPP among the sampling sites were smaller than that of measured biomass. The reason is that measured NPP reflects the annual growth of biomass while measured biomass reflects the accumulated mass of vegetation since the stand establishment. The measurements of biomass and NPP of this study agree well with the results published by Feng et al. (1998). The total errors of the measurements range between 14 and 45 $tDW\,ha^{-1}$ for biomass and between 0.7 and 1.5 $tC\,ha^{-1}\,a^{-1}$ for NPP, respectively.

As a process model, BEPS needs many input parameters, some of which change with the location of the study area. The BEPS model was designed originally for the boreal forest, thus some parameters need to be modified to extend the application of this model to other vegetation types. The experiment results of this study indicate that these modifications are appropriate and that modified BEPS model can be applied effectively to coniferous forests in this study area.

Parameters for NPP modeling vary with vegetation types. The results indicate that for modeled NPP a large difference exists between coniferous forest and other types of vegetation. Therefore, accurate land cover data with precise identification of vegetation types are required to achieve satisfactory modeling results and regional NPP estimates.

LAI with high temporal resolution is a key parameter in the BEPS model. Most of the previous studies used coarse spatial resolution data for NPP estimation. With the limitations of the spatial resolution of LAI, it is a challenge to obtain high spatial resolution NPP data product. The results of this study demonstrate that using the MODIS time series to extend ASTER temporal coverage, and to simulate NPP in finer spatial resolution, is a feasible approach.

The impact of meteorological factors on NPP is more obvious in the area where they limit vegetation growth. Interpolation is always used to transform meteorological data from point data in stations to certain sizes of cells. In previous research, traditional methods such as bilinear interpolation have been used to transform the meteorological data (Liu et al., 2002; Bunkei and Masayuki, 2002). Such interpolated results could be biased in mountainous areas, thus affecting the accuracy of modeled NPP. In this study, accurate distributions of meteorological data were obtained by the combination of ANUSPLIN that incorporated terrain information and bilinear interpolation method.

To overcome the problem of insufficient radiation data from meteorological stations, the NCAR archived data proved to be a valuable data source. The established relationship between global radiation data from NCAR and meteorological stations is similar to those in other studies (Liu et al., 2002). With this relationship the NCAR data could be satisfactorily corrected for use in the BEPS model.

Validation of NPP simulation from coarse spatial resolution data has been a difficult task because of the scale differences between ground measurements and modeling pixels. With the combination of high spatial resolution and temporally frequent remote sensing images, the modeled 15 m NPP simulations can be effectively validated by the ground measurements. BEPS-modeled

NPP values agreed well with ground-measured NPP of forests with high a correlation coefficient (0.84) and low mean relative error (13.9%).

Acknowledgments

The study was funded by the CIDA project and the National Natural Science Foundation of China (nos. 40271081 and 40571109). The authors thank Dr. Julia Pan, Dr. Mingzhen Chen, and Dr. Weiming Ju of the University of Toronto and Dr. Xianfeng Feng in the Institute of Geographical Sciences and Natural Resources Research, China for their great help. Helpful comments and suggestions from two anonymous reviewers are greatly appreciated. The authors also wish to thank all people who participated in the field experiment including Jiangtao Li, Li Li, Donghui Xie, Jiacong Hu, Yonggang Gao, and Yufei Xin.

References

Ahl, D.E., Gower, S.T., Mackay, D.S., Burrows, S.N., Norman, J.M., Diak, G.R., 2004. Heterogeneity of light use efficiency in a northern Wisconsin forest: implications for modeling net primary production with remote sensing. Remote Sensing of Environment 93, 168–178.

Bunkei, M., Masayuki, T., 2002. Integrating remotely sensed data with an ecosystem model to estimate net primary productivity in East Asia. Remote Sensing of Environment 81, 58–66.

Chen, J.M., 1999. Spatial scaling of a remotely sensed surface parameter by contexture. Remote Sensing of Environment 69, 30–42.

Chen, J.M., Liu, J., Cihlar, J., Goulden, M.L., 1999. Daily canopy photosynthesis model through temporal and spatial scaling for remote sensing applications. Ecological Modelling 124, 99–119.

Chen, L.J., Liu, G.H., Feng, X.F., 2001. Estimation of net primary productivity of terrestrial vegetation in China by remote sensing. Acta Botanica Sinica 43 (11), 1191–1198.

Chen, L.J., Liu, G.H., Li, H.G., 2002a. Estimating net primary productivity of terrestrial vegetation in China using remote sensing. Journal of Remote Sensing 6 (2), 129–136.

Chen, J.M., Pavlic, G., Brown, L., et al., 2002b. Derivation and validation of Canada-wide coarse-resolution leaf index maps using high-resolution satellite imagery and ground measurements. Remote Sensing of Environment 80 (1), 165–184.

Chen, J.M., Liu, J., Leblanc, S.G., Lacaze, R., Roujean, J.L., 2003. Multi-angular optical remote sensing for assessing vegetation structure and carbon absorption. Remote Sensing of Environment 84, 516–525.

Choudhury, B.J., 2000. Carbon use efficiency, and net primary productivity of terrestrial vegetation. Advances in Space Research 26 (7), 1105–1108.

Choudhury, B.J., 2002. A biophysical process based approach for estimating net primary production using satellite and ground observations. Advances in Space Research 30 (11), 2505–2510.

Coops, N.C., Waring, R.H., Brown, S.R., Running, S.W., 2001. Comparisons of predictions of net primary production and seasonal patterns in water use derived with two forest growth models in Southwestern Oregon. Ecological Modelling 142, 61–81.

Feng, Z.W., Wang, X.K., Wu, G., 1998. Biomass and Primary Productivity of Forest Ecosystems in China. Science Press, Beijing (in Chinese).

Field, C.B., Randerson, J.T., Malmstrom, C.M., 1995. Global net primary production: combining ecology and remote sensing. Remote Sensing of Environment 51, 74–88.

Furumi, S., Muramatsu, K., Ono, A., Fujiwara, N., 2002. Development of estimation model for net primary production by vegetation. Advances in Space Research 30 (11), 2517–2522.

Geng, Y.B., Dong, Y.S., Meng, W.Q., 2000. Progresses of terrestrial carbon cycle studies. Process in Geography 19 (4), 297–306.

Goetz, S.J., Prince, S.D., 1996. Remote sensing of net primary production in boreal forest stands. Agricultural and Forest Meteorology 78, 149–179.

Gower, S.T., Kucharik, C.J., Norman, J.M., 1999. Direct and indirect estimation of leaf area index, fapar, and net primary production of terrestrial ecosystems. Remote Sensing of Environment 70, 29–51.

Jiang, H., Peng, C.H., Michael, J.A., Zhang, Y.L., Paul, M.W., Wang, Z.M., 1999. Modelling the net primary productivity of temperate forest ecosystems in China with a GAP model. Ecological Modelling 122, 225–238.

Ke, J.H., Piao, S.L., Fang, J.Y., 2003. NPP and its spatio-temporal patterns in the Yangtze River watershed. Acta Phytoecologica Sinica 27 (6), 764–770.

Li, D.Q., Sun, C.Y., Zhang, X.S., 1998. Modelling the net primary productivity of the natural potential vegetation in China. Acta Botanica Sinica 40 (6), 560–566.

Liu, J., Chen, J.M., Cihlar, J., Park, W.M., 1997. A process-based boreal ecosystem productivity simulator using remote sensing inputs. Remote Sensing of Environment 62, 158–175.

Liu, J., Chen, J.M., Cihlar, J., Chen, W., 1999. Net primary productivity distribution in the BOREAS region from a process model using satellite and surface data. Journal of Geophysical Research 104 (D22), 27735–27754.

Liu, J., Chen, J.M., Cihlar, J., Chen, W., 2002. Net primary productivity mapped for Canada at 1-km resolution. Global Ecology and Biogeography 11, 115–129.

Luo, T.X., Li, W.H., Leng, Y.F., Yue, Y.Z., 1998. Estimation of total biomass and potential distribution of net primary productivity in the Tibet plateau. Geographical Research 17 (4), 337–344.

Ni, J., 1996. Estimate of the net primary productivity for subtropical evergreen broadleaved forest in China. Chinese Journal of Ecology 15 (6), 1–8.

Ni, J., 2003. Net primary productivity in forests of China: scaling-up of national inventory data and comparison with model predictions. Forest Ecology and Management 176, 485–495.

Piao, S.L., Fang, J.Y., 2002. Terrestrial net primary production and its spatio-temporal patterns in Qinghai-Xizhang Plateau, China during 1982–1999. Journal of Natural Resources 17 (3), 373–380.

Piao, S.L., Fang, J.Y., Guo, Q.H., 2001. Application of CASE model to the estimation of Chinese terrestrial net primary productivity. Acta Phytoecologica Sinica 25 (5), 603–608.

Reich, P.B., Turner, D.P., Bolstad, P., 1999. An approach to spatially distributed modeling of net primary production (NPP) at the landscape scale and its application in validation of EOS NPP products. Remote Sensing of Environment 70, 69–81.

Sun, R., Zhu, Q.J., 2000. Distribution and seasonal change of net primary productivity in China from April, 1992 to March, 1993. Acta Geographica Sinica 55 (1), 36–45.

Sun, R., Zhu, Q.J., 2001. Estimation of net primary productivity in China using remote sensing data. Journal of Geographical Sciences 11 (1), 14–23.

Tian, Y., Woodcock, C.E., Wang, Y., Privette, J.L., Shabanov, N.V., Zhou, L., Zhang, Y., Buermann, W., Dong, J., Veikkanen, B., Häme, T., Ozdogan, M., Knyazikhin, Y., Myneni, R.B., 2002a. Multiscale analysis and validation of MODIS LAI product over Maun, Botswana, I. Uncertainty assessment. Remote Sensing of Environment 83, 414–430.

Tian, Y., Woodcock, C.E., Wang, Y., Privette, J.L., Shabanov, N.V., Zhou, L., Zhang, Y., Buermann, W., Dong, J., Veikkanen, B., Häme, T., Ozdogan, M., Knyazikhin, Y., Myneni, R.B., 2002b. Multiscale analysis and validation of MODIS LAI product over Maun, Botswana, II. Sampling strategy. Remote Sensing of Environment 83,431–441.

Xiao, Q.G., Chen, W.Y., Sheng, Y.W., Guo, L., 1996. Estimating the net primary productivity in China using meteorological satellite data. Acta Botanica Sinica 38 (1), 35–39.

Zhang, N., Yu, G.R., Zhao, S.D., Yu, Z.L., 2003a. Ecosystem productivity process model for landscape based on remote sensing and surface data. Chinese Journal of Applied Ecology 14 (5), 643–654.

Zhang, N., Yu, G.R., Yu, Z.L., Zhao, S.D., 2003b. Analysis on factors affecting net primary productivity distribution in Changbai Mountain based on process model for landscape scale. Chinese Journal of Applied Ecology 14 (5), 659–664.

Zheng, Y.R., Zhou, G.S., 2000. A forest vegetation model based on NDVI. Acta Phytoecologica Sinica 24 (1), 9–12.

Zhou, G.S., Zhang, X.S., 1995. A natural vegetation NPP model. Acta Phytoecologica Sinica 3, 193–200.

Zhou, G.S., Wang, Y.H., Jiang, Y.L., Yang, Z.Y., 2002. Estimating biomass and net primary production from forest inventory data: a case study of China's Larix forest. Forest Ecology and Management 169, 149–157.

Zhu, Z.H., 1993. A model for estimating net primary productivity of natural vegetation. Chinese Science Bulletin 38 (15), 1422–1426.